JOURNAL OF MAGNETIC RESONANCE **125,** 120–131 (1997)
ARTICLE NO. MN971107

Measurement of the Degree of Coupled Isotopic Enrichment of Different Positions in an Antibiotic Peptide by NMR

A.-F. MILLER,* L. A. EGAN, AND C. A. TOWNSEND

Department of Chemistry, The Johns Hopkins University, Baltimore, Maryland 21218

Received October 21, 1996; revised December 23, 1996

An experimental strategy for determining the extent to which multiply isotopically labeled fragments are incorporated intact into relatively complicated compounds of interest is presented. The NMR methods employed are based on isotope-filtered one-dimensional spectra and difference HSQC spectra incorporating a spin echo designed to report on the presence of a second NMR active isotope at a coupled site. They supplement existing methods for determining the extent of isotopic incorporation at individual sites to reveal whether two coupled labeled sites in a precursor are incorporated as an intact unit into products. The methods described also circumvent ^{1}H signal overlap and distinguish between the effects of different nitrogens coupled to individual carbons. The somewhat complicated case of valclavam illustrates the method's utility in measuring the J coupling constants between ^{13}C and nearby sites that are only fractionally labeled with ^{15}N, and measuring the fraction of molecules in which ^{13}C is coupled to ^{15}N, at each of several sites. The ^{15}N of [2-^{13}C, ^{15}N]-labeled glycine is found to be incorporated into all three N positions of valclavam but most heavily into the N11 position. Specifically, ^{15}N and ^{13}C are incorporated into the N11 and C10 positions together as an ^{15}N^{13}C fragment approximately 8% of the time, whereas ^{15}N is incorporated largely independently at the other positions.

INTRODUCTION

Isotope enrichment and isotope tracing studies are valuable methods for determining the metabolic fates of compounds, and similarly for identifying the metabolic precursors of compounds of interest (*1, 2*). Although mass spectrometry and radioactive label incorporation can be used to determine the extent of isotope incorporation into a compound, except in isolated cases of favorable fragmentation they do not reveal which site is labeled.

NMR spectroscopy can provide information as to what sites have been labeled with NMR active isotopes, and to what degree (*3*). NMR can also reveal the fraction of molecules in which a labeled site is close to another labeled site, via the J coupling between them. Such information is especially valuable as it reveals what (labeled) molecular fragments are incorporated intact and thus represent *bona fide* precursors. In this case, the two coupled sites of the product that are both derived from the fragment would tend to both be labeled, and the probability that the second site is labeled given that the first is labeled will be higher than the overall probability that the second is labeled. Alternately, if the two labels from the fragment are incorporated into the product independently after metabolic transformation, then the likelihood of labeling at the second site is independent of labeling at the first site. In this case, the probability that the second site is labeled given that the first is labeled will be the same as the overall probability that the second site is labeled, and coupled pairs will occur at a frequency which is simply the product of the frequencies of labeling at each of the two sites. Thus, by comparing the frequency with which the second site is labeled over all with the frequency with which it is labeled given that the first site is labeled, one can determine whether the two sites are incorporated into the product as a unit.

In cases where the coupling between coupled sites is large and the level of label incorporation is relatively high, the NMR signals of each site will be seen to be split by the coupling to the other. However, in many circumstances the label is incorporated into the product relatively inefficiently, or is too expensive to be incorporated in large quantity. Second, in complex metabolites the signals from different sites may overlap with one another, complicating the analysis. The latter obstacle is normally resolved by the use of selective pulses and magnetization transfer, or two-dimensional NMR spectroscopy.

A simple variant of the first increment of the ^{13}C^{1}H HMQC has been used to distinguish between small molecules with and without ^{15}N at a given position by allowing ^{13}C to evolve under coupling to ^{15}N for a period of $1/2J$, with the result that the signal intensity is either 1 or 0 depending on whether the ^{13}C is coupled to ^{15}N (*4*). We have doubled the sensitivity of this experiment to ^{15}N by employing a constant time ^{13}C evolution period of $1/J$, resulting in signals of amplitude 1 or -1 for ^{13}C not coupled or cou-

* To whom correspondence should be addressed.

1090-7807/97 $25.00

pled to ^{15}N, respectively, and also included ^{13}C chemical-shift evolution in the constant time delay to obtain signal dispersion in 2D (*5, 6*).

A more fundamental limitation on the measurement of coupled isotope incorporation is imposed by unknown and small *J* couplings arising either because low gyromagnetic ratio nuclei are involved or because the two sites of interest are connected by multiple bonds. In this situation, measurement of *J* by the E.COSY approach (*7, 8*) is limited somewhat by the need for very high resolution in the indirect dimension in order to resolve couplings to the indirectly detected nucleus [but see (*9, 10*)]. Moreover, E.COSY-type methods are complicated when a substantial fraction of the sites to which coupling is to be measured are not labeled, as the signal from these sites falls between the coupled multiplet components and obscures their splitting. Methods that decrease the linewidths of the signal components between which *J* is to be measured by using double- and zero-quantum coherences to encode *J* can ameliorate this problem (*11*), but only to a point. In order to employ weak coupling between heteronuclei to measure the degree of simultaneous labeling, we have used the ''quantitative *J* correlation'' method (*12, 13*) in which the intensity of a resonance from one nucleus provides indirect information on the magnitude of coupling to a second (passively coupled) site, in 1D spectra or relatively low-resolution 2D spectra. Although many NMR experiments have been developed for measuring *J* couplings in proteins and nucleic acids, these generally assume that the two sites of interest are both fully labeled (*12, 14–17*). We have extended the strategies used in the spin-echo-type quantitative *J* correlation experiments to make simultaneous measurements of the magnitude of small *J* couplings and the degree of fractional labeling at a coupled site.

Finally, our method also permits independent measurement of the fractional labeling of two different secondary sites both coupled to the same labeled first site by exploiting the different *J* couplings to, or resonant frequencies of, the different secondary sites. Although the current work observes aliphatic $^{1}H^{13}C$ sites and measures effects due to coupled ^{15}N sites (the ''secondary sites''), our method is equally applicable to other combinations of nuclei, or even to two sites at which the same nucleus resonates in different frequency ranges which can be distinguished by selective pulses. We illustrate our method for the case of the antibiotic peptide valclavam (Fig. 1), produced by *Streptomyces antibioticus* fed [2-^{13}C, ^{15}N] glycine, in order to determine whether this amino acid might be a primary precursor of valclavam. Although relatively small, valclavam nonetheless represents a challenging case because two carbon (C) positions of interest have overlapping ^{1}H signals, and one of these is coupled to two nitrogen (N) sites at once whose resonant frequencies were not known. Despite limited sample availability, our method yields reliable measures of the fraction of ^{13}C coupled to ^{15}N, for each of the C sites independently, and for each of the possible ^{15}N coupling partners, thus providing information on the biosynthetic pathway of valclavam in *S. antibioticus.*

METHODS

Sample Preparation and NMR Spectroscopy

[^{13}C, ^{15}N]-labeled valclavam was produced by fermentation of *S. antibioticus* Tü 1718 (*18*) in a modified soy medium as described elsewhere (*19*). The onset of clavam production was detected by imidazole derivatization and UV assay (*20, 21*) and marked the first of two equal administrations of filtration-sterilized [2-^{13}C, ^{15}N] glycine (1 g total, 7.2 m*M;* Isotech), 53 and 62 h after innoculation. After 121 h, isotopically enriched valclavam was isolated from the fermentation broth as previously described and purified by HPLC to greater than 95% purity (*19*).

Fourteen milligrams of valclavam dissolved in $^{2}H_2O$ was acidified by adjusting the pD to 1.6 with 15% DCl [uncorrected pH electrode reading of 1.2 (*22*)]. The NMR signals of valclavam disappeared gradually over a period of 10–20 h at 25°C and were replaced by others, ascribed to ''acidified valclavam.'' Based on the NMR spectra, valclavam is presumed to have decomposed predominantly into fragments consisting of C5–C7 and N4–C17 respectively (Fig. 1), plus minor products which are not discussed further because their lower concentrations result in less reliable estimates of label incorporation. The predominant N4–C17 fragment produced appears to be identical to the valcalvam degradation product Tü 1718B (*23*), as discussed below.

NMR spectra were obtained on a Unity*plus* spectrometer at 500 MHz for ^{1}H and 125 MHz for ^{13}C. Spectra were obtained at 25°C, and the chemical-shift standard was internal dioxane at 3.53 ppm for ^{1}H and 66.66 ppm for ^{13}C (see Fig. 2). In addition to 1D spectra, double-quantum-filtered correlation spectroscopy [DQCOSY (*24, 25*)] and constant-time $^{1}H-^{13}C$ heteronuclear single-quantum-coherence [CT-HSQC (*5, 6, 26, 27*)] spectra were obtained with the following parameters. DQCOSY spectra were acquired with spectral widths of 4500 Hz in both dimensions. A total of 1024 complex points in t_2 were acquired in 228 ms, and 340 complex points in t_1 were obtained with States quadrature detection and removal of axial signals to the edges of the spectrum (*28*), 24 scans per increment and a 2 s relaxation delay between scans. The t_1 dimension was extended to 680 complex points by linear prediction and zero filled to 2048 complex points. The t_2 dimension was zero filled to 4096 points, and both dimensions were multiplied by shifted sine-bell functions prior to Fourier transformation.

$^{1}H^{13}C$ CT-HSQC spectra were acquired with spectral widths of 4500 and 10,000 Hz in the ^{1}H and ^{13}C dimensions,

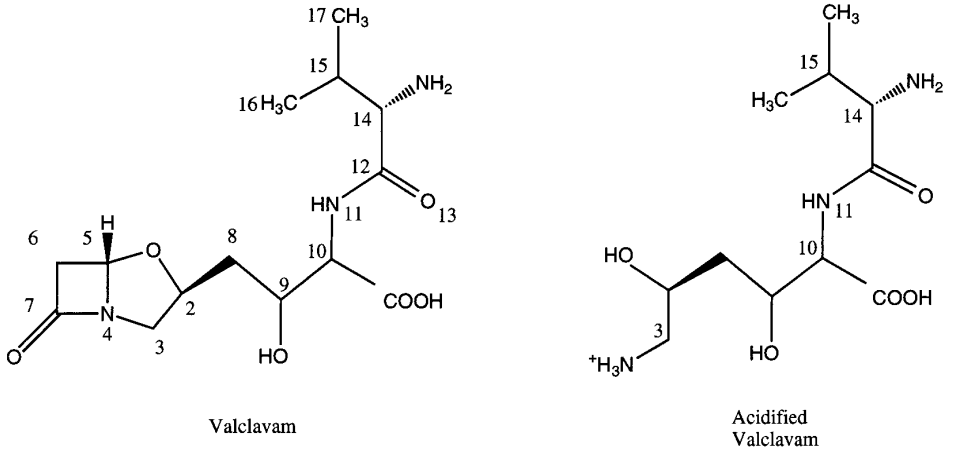

FIG. 1. Structure of valclavam (*23*) and structure of the major fragment formed upon acidification, based on NMR spectroscopy.

respectively. A total of 448 complex t_2 points were acquired in 100 ms with GARP ^{13}C decoupling using a 1.6 kHz decoupling field. A total of 120 complex t_1 points were obtained with quadrature detection and axial signal suppression (*28*), 48 scans per increment and a 2.0 s relaxation delay between scans. A constant time delay of 14.7 ms was used as is customary, despite the fact that coupling between ^{13}C pairs is expected to be very rare due to our use of a singly ^{13}C-labeled glycine precursor and natural-abundance carbon in the other positions. The $1/2J$ delays in the INEPT transfers were set to 3.4 ms to optimize magnetization transfer between ^{13}C and ^{1}H (Fig. 3). The t_1 dimension was extended to 300 complex points by linear prediction and zero filled to 1024 points, the t_2 dimension was doubled by linear prediction and zero filled to 4096 points, prior to multiplication with shifted sine-bell functions in t_1 and t_2, and Fourier transformation.

^{15}N-coupled $^{1}H^{13}C$ CT-HSQC (cpld-HSQC) spectra were acquired and processed similarly to HSQCs, except that constant time delays of 84 to 160 ms were used and pairs of spectra with and without net J coupling to ^{15}N (see below) were interleaved during acquisition.

Assignment of the ^{1}H and ^{13}C Resonances of Valclavam and Acidified Valclavam

DQCOSY spectra were used to assign the ^{1}H resonances of valclavam and acidified valclavam, beginning with the two methyls. A $^{1}H^{13}C$ CT-HSQC spectrum using pulse field gradients to suppress artifacts (*29, 30*) was used to assign the ^{13}C resonances by correlating them with their attached hydrogens. The pulse sequence was modified to include a 6.8 ms interval of net evolution of J coupling between ^{13}C and ^{1}H during the constant time interval (6.8 ms = $1/J_{HC}$). J_{HC}, the coupling constant between ^{1}H and ^{13}C, was found to be very close to 140 Hz for all the $^{13}C^{1}H$ resonances. Thus, the resulting CT-HSQC spectrum displays the resonances of ^{13}C's with an odd number of ^{1}H's attached with the opposite sign to that of the resonances of ^{13}C's with an even number of ^{1}H's, significantly facilitating assignment of the ^{13}C chemical shifts. Figure 2 shows the DQCOSY and the CT-HSQC of acidified valclavam, and Table 1 lists the resonance assignments obtained for valclavam and acidified valclavam. The ^{1}H and ^{13}C chemical shifts of acidified valclavam are all within 0.01 and 0.2 ppm, respectively, of those reported for Tü 1718B in acid solution (*23*), taking into account the systematic differences of 0.22 and 3.0 ppm, respectively, attributable to our use of a different chemical-shift standard with less pH-sensitive resonances (*31*).

In valclavam, the linewidth of the ^{13}C resonance of C10 is significantly larger than the coupling to attached ^{15}N ($\sim$120 vs 12 Hz), so that the amount of attached ^{15}N is difficult to measure accurately. However, the signal of C10 is sharp in acidified valclavam and acidification is not expected to cause ^{15}N to be exchanged between the different positions. Therefore, we used NMR data obtained from acidified valclavam (below) to infer the amount of ^{15}N present in the different positions of the original sample of valclavam.

Pulse Sequences Used for Indirect Observation of ^{13}C and Its Coupling to ^{15}N

In order to distinguish between ^{13}C's bound to ^{15}N and ^{13}C's bound to ^{14}N or other C's, a CT-HSQC experiment was modified to include ^{15}N 180° pulses positioned in the ^{13}C evolution time so as to ensure either no net evolution of J coupling between ^{13}C and ^{15}N or accumulation of J coupling during the entire constant time interval (Fig. 3). The basic pulse sequence is essentially the $\{^{15}N\}$ spin-echo difference CT-HSQC of Vuister *et al.* (*12*), augmented by the use of gradients to suppress artifacts (*29*) and with the spin lock omitted. A 90° pulse followed by a pulsed field gradient nulls net magnetization of ^{13}C prior to beginning the CT-HSQC experiment proper (time point *a*). After excitation

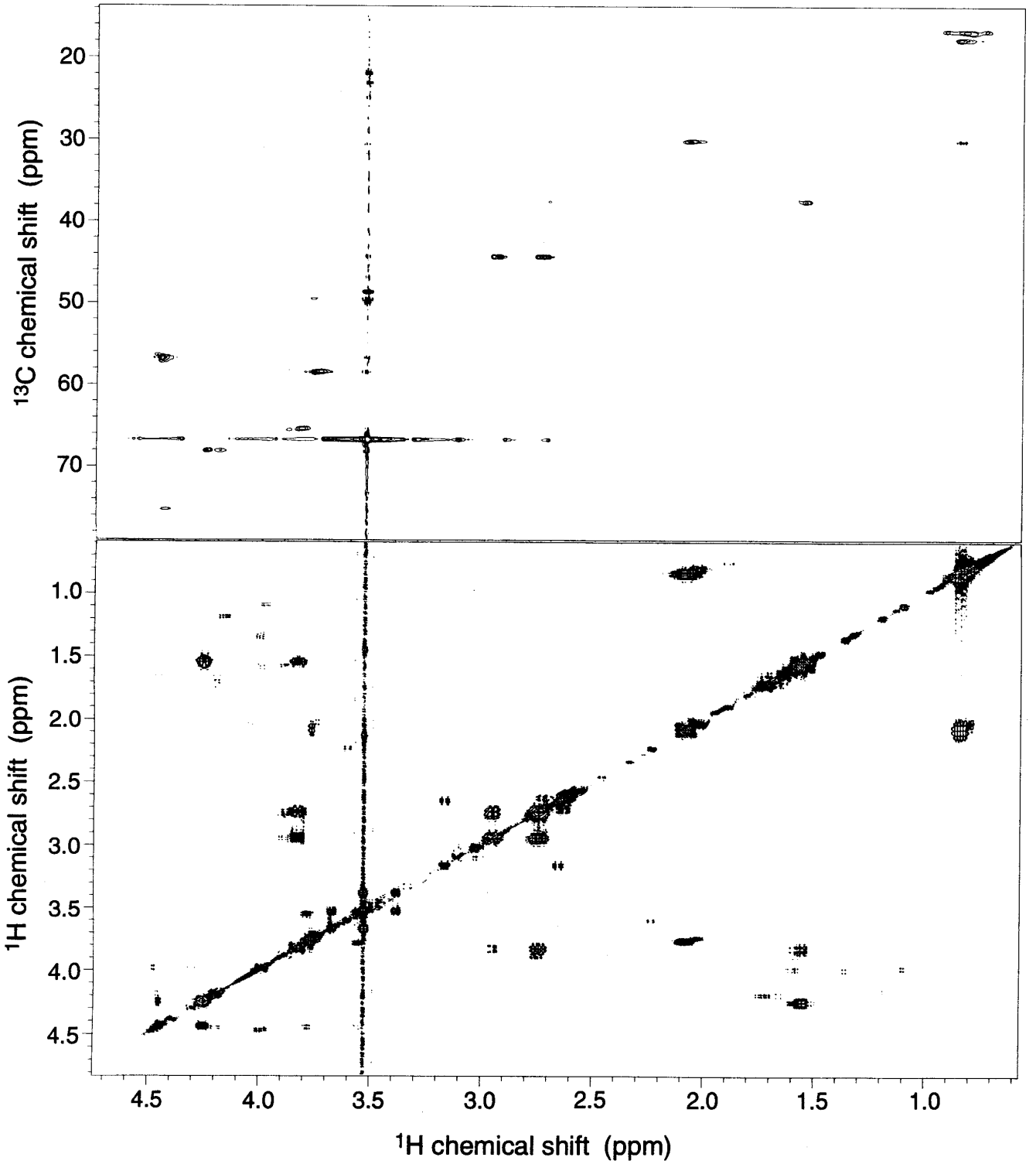

FIG. 2. DQCOSY and CT-HSQC spectra of acidified valclavam, aligned with the same ^{1}H axis. Spectral parameters as under Methods.

of ^{1}H and INEPT transfer of net magnetization to ^{13}C (*32*), the antiphase ^{13}C magnetization formed at time point *b* evolves according to the ^{13}C chemical shift during $t_1 = t_a + t_b - t_c$, during the constant time (CT) delay of CT = $t_a + t_b + t_c$. There is no net accumulation of *J* coupling to ^{1}H in this case, as we maintain $t_b = t_a + t_c$. Thus, ^{13}C magnetization

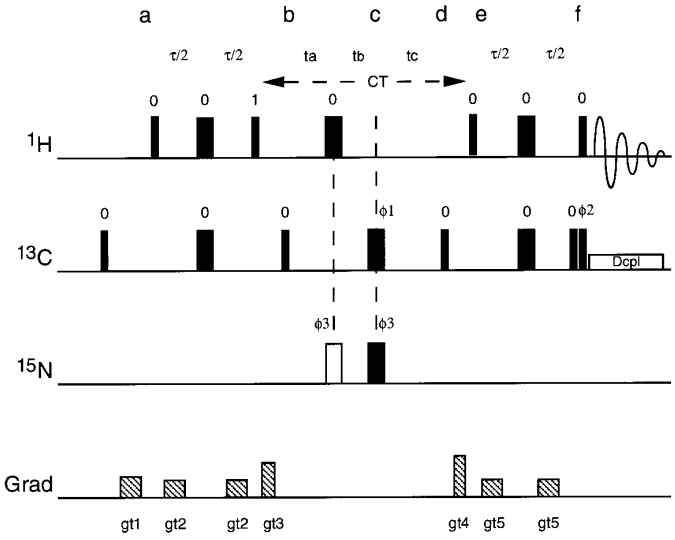

FIG. 3. Pulse sequence of cpld-HSQC showing the ^{15}N pulse that leads to net coupling between ^{15}N and ^{13}C during CT [also see (*12*)]. Narrow bars indicate 90° pulses, wide bars indicate 180° pulses. For the ^{15}N pulses, the filled symbol indicates the pulse that is used to ensure net J coupling between ^{13}C and ^{15}N during all of CT, the open symbol indicates the pulse that is used instead to ensure no net coupling between ^{13}C and ^{15}N during CT. The phase cycle used was $\phi1 = 0, 1, 2, 3$; $\phi2 = 4 \times 0, 4 \times 2$; $\phi3 = 8 \times 0, 8 \times 2$; receiver = 0, 2. All other pulse phases are indicated. $\tau = 3.4$ ms, $t_a = t_1/2$, $t_b = \mathrm{CT}/2$, $t_c = \mathrm{CT}/2 - t_1/2$. Gradients used were gt1, 0.5 ms and 5 G/cm; gt2, 0.3 ms and 3 G/cm; gt3, 1.5 ms and 15 G/cm; gt4, 0.6 ms and −10 G/cm; gt5, 0.2 ms and 2 G/cm.

remains antiphase with respect to ^{1}H at time point *d* and is returned to ^{1}H antiphase magnetization at time point *e* by a pair of 90° pulses. The reverse INEPT sequence refocuses ^{1}H magnetization with respect to ^{13}C, yielding observable in-phase ^{1}H magnetization at time point *f*. Two more ^{13}C pulses and an ^{1}H pulse serve to eliminate signals from ^{1}H not coupled to ^{13}C (*33*) and signals from ^{1}H magnetization antiphase to ^{13}C at the end of the INEPT transfer (*34*). This sequence selects only magnetization that passes through ^{13}C, thus selecting only ^{1}H coupled to ^{13}C for observation. In order to accumulate J coupling between ^{13}C and ^{15}N during the entire constant time interval CT, a 180° pulse is applied to ^{15}N simultaneously with the 180° pulse on ^{13}C (time point *c*). Thus, although chemical-shift evolution of ^{13}C is reversed by the 180° pulse on ^{13}C, the ^{15}N pulse ensures that J coupling to ^{15}N continues to accumulate. J coupling between ^{13}C and ^{15}N accumulates throughout the constant time interval regardless of whether the sequence is used to collect 1D ^{13}C-edited ^{1}H spectra or 2D CT-HSQC spectra. Only ^{13}C magnetization in phase with respect to ^{15}N leads to observable ^{1}H magnetization, so for each resonance whose ^{13}C is coupled to ^{15}N, the signal intensity is proportional to $\cos(\pi J_{\mathrm{CN}}\mathrm{CT})$, where J_{CN} is the appropriate ^{13}C–^{15}N coupling constant. (The related sine component associated with antiphase ^{13}C magnetization is not observed.) Resonances whose ^{13}C is not coupled to ^{15}N are not affected by the ^{15}N pulse and retain their full intensity.

Control spectra with no net evolution of J coupling between ^{15}N and ^{13}C were acquired using a pulse sequence in which the ^{15}N pulse at point *c* is omitted and a 180° pulse is applied to ^{15}N simultaneously with the 180° pulse on ^{1}H instead (open symbol, Fig. 3), so that J_{CN} evolves in opposite directions during equal periods of time ($t_a + t_c = t_b$). This ^{15}N pulse is unnecessary when 1D spectra are collected, as t_1 is zero, so that $t_a = 0$ and $t_b = t_c$. In 2D CT-HSQC spectra, t_a is incremented to nonzero values and in the absence of a 180° ^{15}N pulse, net J_{CN} coupling accumulates during t_1. However, since J_{CN} is comparable to or smaller than the ^{13}C resolution in the 2D spectra ($J_{\mathrm{CN}} < 15$ Hz vs $\approx$10 Hz/point), and the maximum value of t_1 is only a fraction of CT ($\leqslant$13 ms vs CT $\geqslant$ 84 ms), the effect of J_{CN} in t_1 is very small. Moreover, since the integrated intensity of the peak produced after Fourier transformation of the ^{13}C dimension depends only on the amplitude of the signal in the $t_1 = 0$ increment, the same peak volumes should be obtained in the resulting CT-HSQC spectra regardless of whether an ^{15}N pulse is applied during t_1. We have collected ''no net coupling'' spectra with and without a refocusing ^{15}N pulse during t_1, and the peak volumes obtained by the two methods were not significantly different. In these control spectra, ^{13}C coupled to ^{15}N and ^{13}C coupled to ^{14}N (or ^{13}C not coupled to N) peak volumes are not affected by J_{CN}.

One-dimensional versions of the experiment with and without net coupling to ^{15}N were also collected. These selectively observe only those protons bound to ^{13}C, but, in order to avoid errors due to residual signal from ^{1}H bound to ^{12}C, the ^{1}H spectra were not ^{13}C decoupled with the result that

TABLE 1
Resonance Assignments for Valclavam and Acidified Valclavam[a]

Valclavam			Acidified Valclavam		
Position	δH (ppm)	δC (ppm)	Position	δH (ppm)	δC (ppm)
2	4.39	79.56	2	3.83	65.25
3	3.94	50.38	3	2.74	44.08
3	2.69	50.38	3	2.95	44.08
5	5.35	84.01			
6	3.30	44.44			
6	2.86	44.44			
8	1.72	36.78	8	1.56	37.45
8	1.83	36.78	8	1.56	37.45
9	4.11	69.00	9	4.25	67.81
10	4.16	59.51	10	4.46	56.53
14	3.84	45.44	14	3.77	58.27
15	2.19	29.92	15	2.08	30.00
16	0.96	16.72	16	0.83	16.62
17	0.98	17.77	17	0.86	17.55

[a] Chemical shifts are relative to dioxane at 3.53 ppm ^{1}H and 66.66 ppm ^{13}C.

the signals of interest from ^{1}H bound to ^{13}C appeared $0.5J_{CH}$ Hz on either side of the small but occasionally significant residual signal from ^{1}H bound to ^{12}C.

Calculation of the Fraction of ^{13}C Bound to ^{15}N

In both the net coupling and no net coupling experiments, magnetization remains on ^{13}C for the same amount of time (CT) regardless of how much of that time is used for chemical-shift evolution (t_1). Thus, in addition to the factors described above, the intensity with which each resonance is observed depends on $(\sin \pi J_{HC}\tau)^2 \times e^{-CT\times R}$, where $\sin(\pi J_{HC}\tau)$ describes the efficiency of each INEPT transfer, R is the relaxation rate of antiphase ^{13}C magnetization during CT, and τ is the INEPT delay, chosen approximately equal to $1/2J_{HC}$. We neglect relaxation during the relatively short delays τ, but relaxation is considered for the CT delay, as this is considerably longer (up to 125 ms, vs 6.8 ms for 2τ). We assume that ^{13}C magnetization that is antiphase with respect to ^{1}H and ^{15}N relaxes at a rate similar to that of ^{13}C magnetization that is antiphase with respect to only ^{1}H, as the former's relaxation rate is roughly equal to the latter's plus $1/T_{1N}$, which is smaller than $1/T_{1H}$ or $1/T_{2C}$ for a small molecule like valclavam at 500 MHz. Thus, the above factors are not much changed by the presence or position of the pulse on ^{15}N and are written together as a constant $Q = (\sin \pi J_{HC}\tau)^2 \times e^{-CT\times R}$ for each resonance.

Assuming that the ^{15}N pulse during CT is on resonance, the difference between the signal intensities produced with no net J_{CN} coupling (control) and with net J coupling is

$$\begin{aligned}\Delta(\text{control} - J\ \text{coupled}) &= Q(\#\text{not bound to } ^{15}\text{N} + \#\text{bound to } ^{15}\text{N}) \\ &\quad - Q[(\#\text{not bound to } ^{15}\text{N}) + (\#\text{bound to } ^{15}\text{N}) \\ &\quad \times \cos(\pi J_{CN}\text{CT})] \\ &= Q[1 - \cos(\pi J_{CN}\text{CT})](\#\text{bound to } ^{15}\text{N}), \end{aligned} \quad [1]$$

where the spin populations ''not bound to ^{15}N'' and ''bound to ^{15}N'' specify the two categories of ^{13}C distinguished by the experiment. For each resonance, the constant Q cancels out upon division of this difference by the signal intensity in the control spectrum

$$\begin{aligned}\frac{\Delta(\text{control} - J\ \text{coupled})}{\text{control}} &= (1 - \cos \pi J_{CN}\text{CT}) \\ &\quad \times \frac{(\#\text{bound to } ^{15}\text{N})}{(\#\text{not bound to } ^{15}\text{N}) + (\#\text{bound to } ^{15}\text{N})} \\ &= (1 - \cos \pi J_{CN}\text{CT})F_{(C,N)}, \end{aligned} \quad [2]$$

where $F_{(C,N)}$ is the fractional ^{15}N labeling, given that the C position is labeled with ^{13}C.

Finally, for ^{15}N with a resonant frequency very different from the carrier frequency used, a pulse of less than 180°, or effectively $180° - \theta$, is felt. It is easy to show that the intensity observed for a CH bound to ^{15}N is now reduced, not by a factor of $\cos(\pi J_{CN}\text{CT})$ as above, but only by a factor of

$$\left[\cos(\pi J_{CN}\text{CT}) \times \left(1 - \frac{(1 - \cos\theta)}{2}\right) + \frac{(1 - \cos\theta)}{2}\right]$$

when there is net coupling to ^{15}N. Thus, in general with $\chi = (1 - (1 - \cos\theta)/2)$,

$$\begin{aligned}\frac{\Delta(\text{control} - J\ \text{coupled})}{\text{control}} &= \chi(1 - \cos \pi J_{CN}\text{CT})F_{(C,N)}. \end{aligned} \quad [3]$$

$\chi = 1$ for those ^{13}C^{1}H with a bound ^{15}N which is on resonance and $0 \leqslant \chi \leqslant 1$ for CH's with a bound ^{15}N which is off resonance. In both cases, the correct value for J_{CN} is still obtained. Off-resonance effects could be minimized by using composite ^{15}N inversion pulses. Alternately, long selective ^{15}N pulses could be used to separately measure the J_{CN} and the fraction ^{13}C bound to ^{15}N for ^{13}C's bound to ^{15}N in different spectral regions (in the present case, the amines near 40 ppm and the amides near 120 ppm). However, in practice most samples contain several ^{15}N sites of each type, so that moderately short (composite) pulses are desirable to ensure uniform inversion of each type by the 180° pulses. If typical moderately short ^{15}N pulses are used, both types of ^{15}N respond but the off-resonance ^{15}N is not fully inverted, so that a lower apparent fraction of ^{13}C bound to off-resonance ^{15}N is observed, $\chi F_{(C,N)}$, and experiments may need to be performed twice, with ^{15}N pulses applied to the amine and amide ^{15}N's in turn.

As a test of our method's ability to measure the fraction of ^{13}C bound to ^{15}N, pairs of 1D spectra with and without net coupling of ^{13}C to ^{15}N were obtained of a sample containing a 1:9 ratio of ^{15}N threonine and ^{14}N threonine, both with natural abundance ^{13}C, with the ^{15}N carrier set at the amine frequency and CT = 161 ms. Using $J_{CN} = 6.2$ Hz, as determined from the ^{13}C spectrum of ^{15}N-labeled threonine, the fraction of ^{15}N bound was found to be 9%. (The choice of $CT = 1/J$ maximizes the effect of coupling, fully inverting the signal from sites coupled to ^{15}N relative to the signal from sites not coupled to ^{15}N.) Similarly, a sample containing a 1:5 ratio of ^{15}N threonine to ^{14}N threonine was found to have 21% ^{15}N using CT = 125 ms. These values agree relatively well with the anticipated percentages of 10 and 17%. Thus, the NMR method described above gives moder-

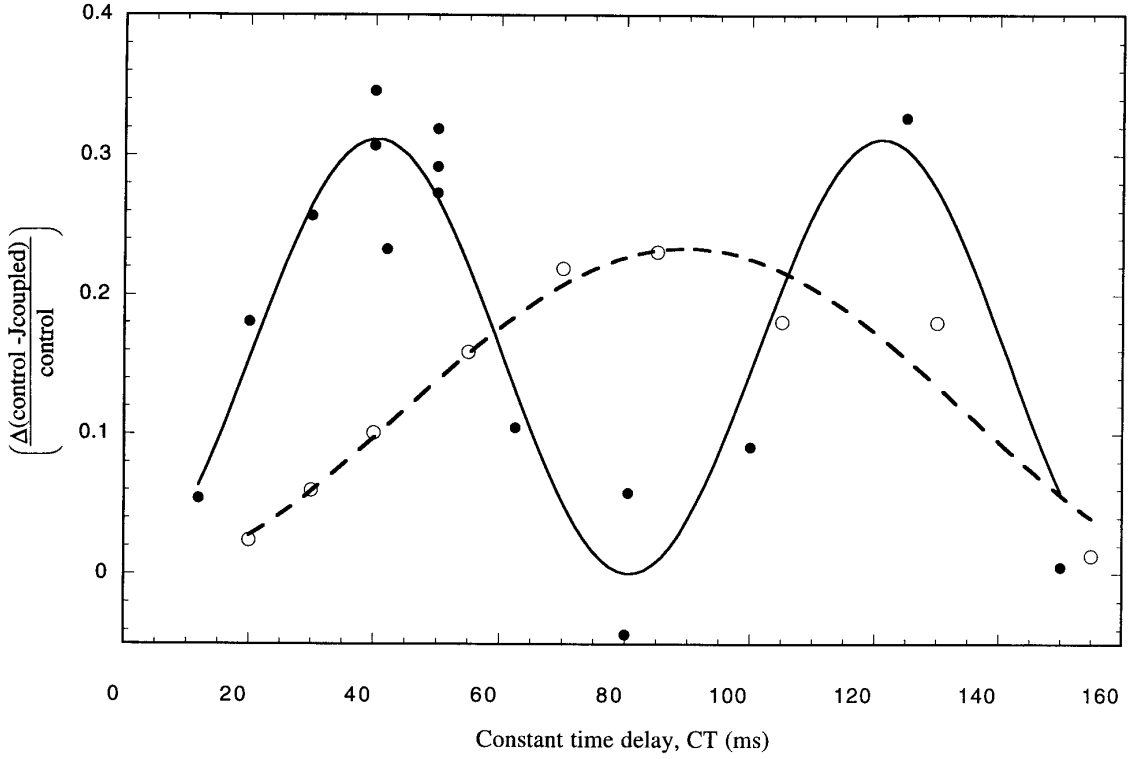

FIG. 4. Plots of (Δ(control − *J* coupled)/control) vs CT and fit of Eq. [3] to the data, for the ^{1}H resonances of C10 at 4.59 ppm (●) and C3 at 2.88 ppm (○) with the ^{15}N pulse applied to the amide and amine ^{15}N's, respectively. One-dimensional cpld-HSQC spectra were collected with and without net coupling to ^{15}N, using a range of CT values. For each resonance of interest, peak heights were measured in the control and net *J* coupled spectra, and (Δ(control − *J* coupled)/control) was calculated for each value of CT, as the ratio of the difference in peak heights to the peak height in the control spectrum. The fits to Eq. [3] were performed using KaleidaGraph 2.0 and yielded J_{CN} = 12.4 and 5.6 Hz, respectively. The proton chemical shifts quoted here are 0.14 ppm ($=J_{HC}/2$) from the values listed in Table 1, because the spectra used here were not decoupled with respect to ^{13}C.

ately accurate measurements of the amount of ^{15}N attached to specific sites even for relatively low fractional enrichments and relatively small *J* couplings between sites. The experiments are also relatively sensitive because they employ ^{1}H excitation and detection, while nonetheless permitting resolution of signals in ^{13}C (and ^{15}N) dimensions. Finally, they also permit measurement of small *J* couplings provided that the T_2's of the nuclei involved are long enough.

RESULTS AND DISCUSSION

Calculation of the Magnitude of J Coupling between Indirectly Observed ^{13}C and ^{15}N

In order to determine the fraction of ^{13}C bound to ^{15}N, one needs to know J_{CN}, the magnitude of the coupling between ^{13}C and ^{15}N, as well as χ. J_{CN} can be measured from the ^{15}N splitting of the ^{13}C signal of interest in the ^{13}C spectrum if substantially ^{15}N-labeled compound is available and the ^{13}C spectrum is well enough resolved. Alternately, one can use the pulse sequence described above and isolate J_{CN} by varying the CT delay with χ and $F_{(C,N)}$ fixed, collecting 1D spectra with and without net coupling to ^{15}N at each value of CT, plotting the ratio of the difference in peak heights to the height without net coupling, Δ(control − *J* coupled)/control, as a function of CT, and fitting the results to Eq. [3].

In principle, this procedure yields estimates of both the magnitude of J_{CN} and χ times the fraction of ^{13}C bound to ^{15}N. However, signals that have the same ^{1}H chemical shifts as signals of interest can contribute to the total peak amplitude in the control spectrum, and thus lead to an underestimate of the fraction of ^{13}C bound to ^{15}N. Such overlapping ^{1}H signals should not affect the value of J_{CN} obtained, unless by chance they also correspond to ^{1}H's bound to ^{13}C bound to ^{15}N with another *J* value (for example, C14 below). Similarly, the value of J_{CN} obtained is independent of the value of χ. The experimental results are expected to be most sensitive to J_{CN} when CT is small ($J_{CN} \times CT \ll \frac{1}{6}$), but most sensitive to χ and $F_{(C,N)}$ when CT is chosen to be approximately $1/J_{CN}$. Thus, for best results, J_{CN} should be obtained from different experiments with shorter CT's than those used to measure χ and $F_{(C,N)}$. These experiments measure the magnitude but not the sign of J_{CN}.

Typical data from acidified valclavam are plotted in Fig. 4 and the results are summarized in Table 2. In the

TABLE 2
Results of Fits of [△(control-*J* coupled)/control] to CT:J_{CN} with Errors[a]

	^{15}N pulses on amide			^{15}N pulses on amine		
Position	Resonance[b] (ppm)	J_{CN} (Hz)	Error (Hz)	J_{CN} (Hz)	Error (Hz)	Average J_{CN}
C10	4.549	12.4	0.2	11.2	0.3	12 Hz
	4.31	11.8	0.1	12.6	0.3	
C14[c]	3.91	8.3	0.2	7.7	0.2	8 Hz
C3[d]	3.08	6.3	0.4	5.9	0.4	6 Hz
	2.79	6.5	0.5	6.2	0.2	
C3[d]	2.88	6.6	0.5	5.6	0.2	
	2.60	6.0	0.4	5.0	0.3	

[a] Data such as those in Fig. 4 were fitted with Eq. [3] using KaleidaGraph 2.0 to obtain the values of J_{CN} and the errors listed here.
[b] Two resonances per signal because ^{13}C is not decoupled during acquisition (see text).
[c] One C14 signal overlaps with dioxane and therefore was not analyzed.
[d] C3 has two protons.

1D experiments, a relatively long ^{1}H acquisition time was used in order to improve resolution, and ^{13}C was not decoupled so that the central residual signal from ^{1}H's bound to ^{12}C would not overlap the signals of interest from ^{1}H bound to ^{13}C. The J_{CN} of 12 Hz obtained for position C10 is close to the value of 11 Hz expected for a C_α and its attached amide ^{15}N based on studies of proteins (*16, 35*). The value of 6 Hz obtained for position C3 is within error of the value of 6.2 Hz observed for coupling of C_α to its attached amine in ^{15}N-labeled threonine. C14 has an effective J_{CN} of 8 Hz but is discussed further below, as it is coupled to two different N's.

2D Spectra and Calculation of the Fraction of ^{13}C Bound to ^{15}N at Positions C10 and C3

Two-dimensional cpld-HSQC spectra were collected in order to resolve signals of interest from others with the same ^{1}H chemical shift on the basis of their different ^{13}C chemical shifts (the protons between 4.4 and 4.5 ppm for example, Fig. 5a). Two different constant-time delays of 84 and 125 ms were used to maximize the effects produced by the J_{CN} values of C10 and C14, respectively, and ^{15}N pulses were applied at 120 ppm for maximum excitation of amide ^{15}N's. For each value of CT, a pair of interleaved cpld-HSQC spectra was obtained, one with and one without net coupling to ^{15}N during CT. In each case the two spectra appeared very similar but the volumes of the peaks of ^{13}C^{1}H's bound to ^{15}N were smaller in the spectrum that reflected net coupling to ^{15}N, whereas other ^{13}C^{1}H resonances were unchanged. Subtraction of the data collected with net coupling to ^{15}N from the data collected without yielded a very clean cpld-HSQC difference spectrum for each of the two values of CT. These difference spectra contain peaks from all the ^{13}C^{1}H positions coupled to an ^{15}N, but none of the others (Fig. 5b). (They also contain noise streaks due to the residual strong dioxane resonance at 3.5 ppm ^{1}H and 66.7 ppm ^{13}C.)

Quantitative interpretation of the difference signals involved measurement of the difference volume and the volume in the absence of net coupling to ^{15}N. These values, the value of CT, and the value of J_{CN} obtained above were used in Eq. [3] to calculate $F_{(C,N)}$ or $\chi F_{(C,N)}$, for ^{15}N on resonance (with $\chi = 1$) or off resonance, respectively (Table 3). This was done for the resonances of positions C10 and C3, which are each bound to a single N. Peak volumes were also measured in the two parent spectra, and their difference was found to be within less than 1% of the peak volume in the difference spectrum. The volume of the peak of C15 which is not attached to ^{15}N was the same in the two parent spectra to within 0.4%, consistent with the absence from the difference spectra of ^{13}C^{1}H's not coupled to ^{15}N and suggesting that the random error is ≈1%. $F_{(C,N)}$, the fraction of ^{13}C bound to ^{15}N, was found to be 0.17 for C10 (bound to an amide), and $\chi F_{(C,N)}$ was found to be 0.06 for C3 (bound to an amine, Table 3). The excellent agreement between values obtained using different values of CT supports the validity of the J_{CN} values used.

Two more pairs of cpld-HSQC spectra were collected using the ^{15}N carrier frequency of 40 ppm appropriate for amine ^{15}N. These also produced clean difference spectra, and the peak volumes were used as above along with the CT values of 125 or 84 ms and the known J_{CN} values to calculate $F_{(C,N)}$ (times χ) for C3 (and C10), using Eq. [3]. $\chi F_{(C,N)}$ was 0.10 for C10 and $F_{(C,N)}$ was 0.12 for C3 (Table 3). Again, values obtained for $F_{(C,N)}$ using different values of CT agree well, supporting the values of J_{CN} used (Table 3). The results obtained using the resonant ^{15}N frequencies of each ^{15}N yield $F_{(C,N)} = 0.17$ for C10 and 0.12 and 0.13 for C3. Two average values are obtained for $F_{(C,N)}$ for the amine attached to C3 as this ^{13}C is observed via two different ^{1}H^{13}C cross peaks. The agreement obtained between these further supports the method.

Determination of χ

The value of χ can be determined by collecting data using a range of carrier frequencies for the secondary site (^{15}N here), with CT and $F_{(C,N)}$ held constant. Thus, the above analyses yielded two different estimates of χ per CH resonance, one from each set of spectra obtained with a given CT but different ^{15}N carrier frequencies. The scatter among the four χ values obtained for C3 provides an empirical estimate of the experimental uncertainty in χ, since a single value of χ is being measured ($\bar{\chi} = 0.50$, $\sigma = 0.06 = 12\%$). The value of χ for an 80 ppm offset

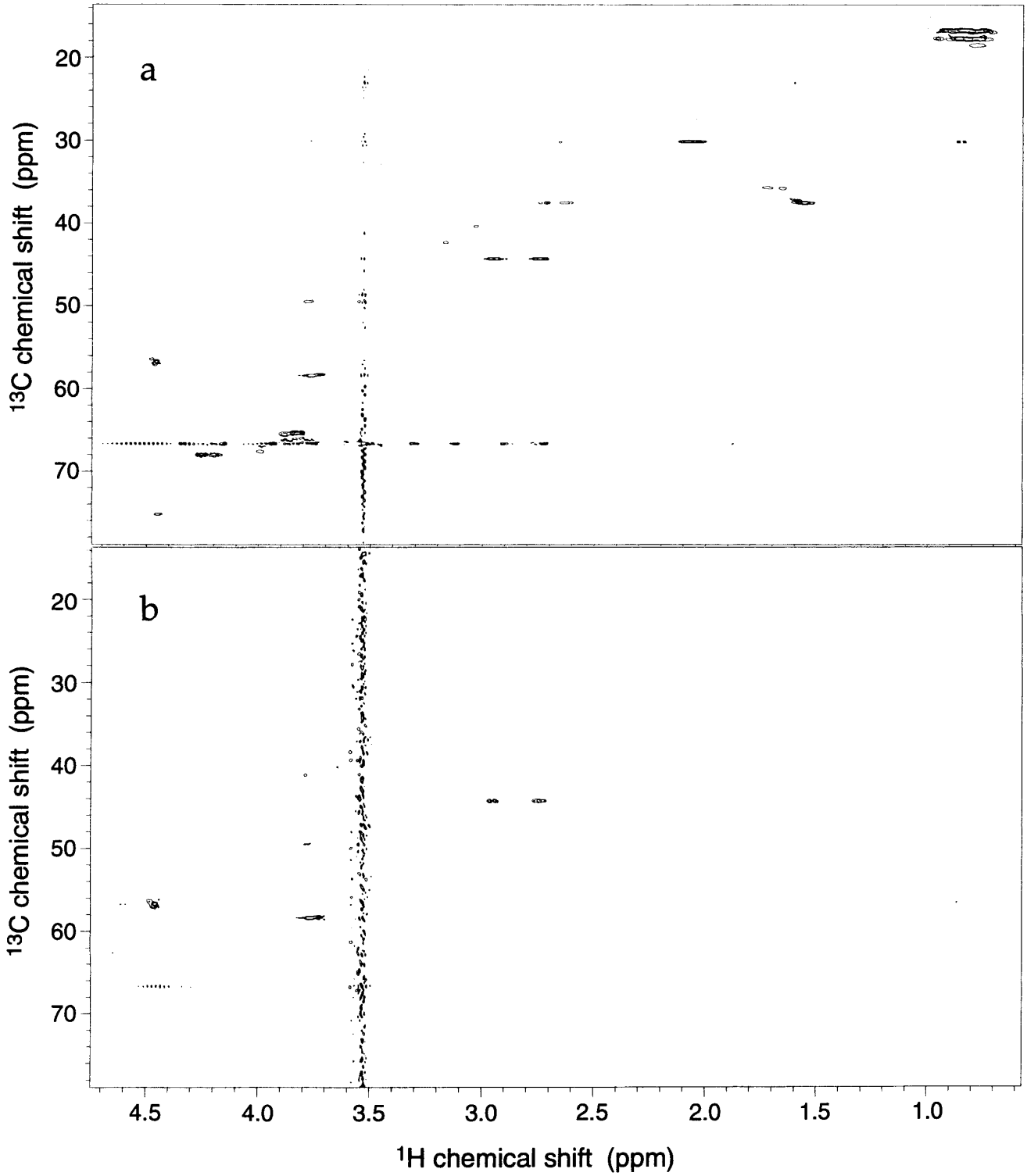

FIG. 5. Cpld-HSQC without net coupling to ^{15}N (a), and difference cpld-HSQC (b) (control − *J* coupled). CT was 84 ms and ^{15}N pulses were applied at 120 ppm. Spectral parameters are as under Methods, and the pair of cpld-HSQC spectra were acquired in 14 h.

from resonance was also determined from 1D experiments conducted on ^{15}N threonine at a range of ^{15}N carrier frequencies. The χ values obtained for C10 and threonine fall within the range of χ values obtained from C3 with one exception (Table 3), indicating that they are all the same within error, consistent with the fact that, in all three cases, off-resonance irradiation is

TABLE 3
Values of J_{CN}, χ, and Fraction of ^{13}C Bound to ^{15}N Obtained for Threonine and the Large Fragment of Acidified Valclavam

		$\chi F_{(C,N)}$									
		^{15}N pulse on amide		^{15}N pulse on amine							
Compound, position	CT =	125 ms	84 ms	125 ms	84 ms		J (Hz)	χ	$\bar{\chi}$	$F_{(C,N)}$	$\overline{F_{(C,N)}}$
Threonine			0.11		0.21		6.2	0.53		0.21	
Acidified valclavam											
C10		0.18	0.16	0.092	0.10		12	0.50, 0.60	**0.55**	0.18, 0.16	**0.17**
C3, 2.95 ppm		0.055	0.059	0.13	0.13		6	0.43, 0.45	**0.50**	0.13, 0.13	**0.12**
C3, 2.74 ppm		0.067	0.064	0.12	0.11		6	0.55, 0.58		0.12, 0.11	
C14		0.29	0.23	0.32	0.23	Amide	9[a]	(0.52)			**0.09**[a]
						Amine	7[a]	(0.52)			**0.12**[a]

[a] Calculated using the known $\chi = 0.52$; see text.

≈80 ppm off resonance, and theory predicts that it does not matter which direction from resonance the irradiation frequency is. Thus, the overall average χ obtained from C10, the two protons attached to C3, and threonine is 0.52, and applicable to amines observed via amide pulses or amides observed via amine pulses in our experiments at 50 MHz for ^{15}N with an 84 μs ^{15}N 180° pulse.

One-dimensional spectra of acidified valclavam were also collected using an array of ^{15}N carrier frequencies in order to characterize the frequency dependence of χ. Although the anticipated qualitative behavior was obtained, the data contained too much scatter and interference from overlapping ^{1}H signals to permit high-quality estimates of χ from 1D spectra in this case.

Determination of the Fraction of ^{13}C Bound to ^{15}N at the Two N Positions near C14

C14 is within coupling range of two different N's, an amine and an amide (N11). Although a single J value of 8 Hz appeared adequate to describe the dependence of net coupling to ^{15}N on the duration of CT in 1D spectra (Table 2), the 2D spectra show that the ^{1}H of another ^{13}C coupled to ^{15}N overlaps with that of C14 in the ^{1}H spectra, so the apparent coupling is not only the weighted average of two couplings to C14, but also reflects coupling between ^{15}N and C6′. (The resonance in question is at 3.77 ppm ^{1}H and 49.43 ppm ^{13}C, and is tentatively assigned to the C6 position in a minor side product of valclavam acidification in which C6 remains bound to N4). Thus we do not know the individual J_{CN} values to the different N's coupled to C14. Moreover, although the fraction of ^{13}C at position 10 that is coupled to ^{15}N at position N11 was found to be 0.17 (above), this is not necessarily the same as the fraction of ^{13}C at position 14 coupled to ^{15}N at N11, or the overall fractional labeling of N11, as these three can vary independently depending on the extent to which $^{13}C-^{15}N$ units are incorporated intact and the positions into which they are incorporated.

However, the contributions of the two different N's coupled to C14 can be distinguished based on their very different resonant frequencies and thus different χ values at a given frequency. For moderate levels of independent ^{15}N incorporation at two sites, the likelihood of a ^{13}C being coupled to two different ^{15}N's at once is the product of the two individual probabilities of labeling, and can be neglected in our case (as the maximimum probability anticipated is $0.17 \times 0.17 = 3\%$). Thus, the effects of coupling of ^{15}N to C14 are approximately the sum of the effect due to ^{15}N in the adjacent amine position plus the effect due to ^{15}N in the more distant amide position. When the ^{15}N frequency is set to the amine frequency, coupling to the amine ^{15}N will have its full effect on the resonance of C14 but coupling to the amide ^{15}N will have only ≈52% of its effect. Conversely, when the ^{15}N frequency is set to the amide frequency, the amine will have only ≈52% of its effect but the amide ^{15}N will have its full effect. Thus, for C14, two pairs of experiments using different ^{15}N carrier frequencies yield two different experimental values for the combined amount of bound ^{15}N, for a given choice of CT

$$\left(\frac{\Delta(\text{control} - J\ \text{coupled})}{\text{control}}\right)_{\text{amine}} = (1 - \cos \pi {}^{1}J_{CN}\text{CT})F_{(C,N)\text{amine}} + \chi(1 - \cos \pi {}^{2}J_{CN}\text{CT})F_{(C,N)\text{amide}} = 2\left(\sin \frac{\pi {}^{1}J_{CN}\text{CT}}{2}\right)^{2} F_{(C,N)\text{amine}} + 2\chi\left(\sin \frac{\pi {}^{2}J_{CN}\text{CT}}{2}\right)^{2} F_{(C,N)\text{amide}} \quad [4a]$$

$$\left(\frac{\Delta(\text{control} - J\ \text{coupled})}{\text{control}}\right)_{\text{amide}} = 2\chi\left(\sin\frac{\pi\,{}^1J_{\text{CN}}\text{CT}}{2}\right)^2 F_{(\text{C,N})\text{amine}} + 2\left(\sin\frac{\pi\,{}^2J_{\text{CN}}\text{CT}}{2}\right)^2 F_{(\text{C,N})\text{amide}}, \quad [4b]$$

where ${}^1J_{\text{CN}}$ and ${}^2J_{\text{CN}}$ are the one-bond coupling to the neighboring amine and the two-bond coupling to the more distant amide, respectively. At least four independent experimental measures of $\Delta(\text{control} - J\ \text{coupled})/\text{control}$ are needed to solve for both values of $F_{(\text{C,N})}$ and both values of J_{CN}. In addition to using two different ^{15}N carrier frequencies to distinguish the contributions of the different sites, we varied CT as well to obtain separate estimates of J_{CN} for the different sites.

With a known value of $\chi = 0.52$, the two equations using the same CT but different ^{15}N frequencies can be combined to eliminate the second (or the first) term on the right, yielding an expression relating $(\sin \pi\,{}^1J_{\text{CN}}\text{CT}/2)^2 F_{(\text{C,N})\text{amine}}$ to a number derived from two experimental values. When this is done for the results obtained with two different CT values, the two expressions can be solved for $F_{(\text{C,N})\text{amine}}$ and ${}^1J_{\text{CN}}$. Thus, we obtain $F_{(\text{C,N})\text{amine}} = 0.12$ and ${}^1J_{\text{CN}} = 7$ Hz. ${}^1J_{\text{CN}}$ is not too far from the value of 6.2 Hz obtained for C_α coupling to the adjacent amine in ^{15}N threonine. When the first term on the right is eliminated and the resulting two expressions for $(\sin \pi\,{}^2J_{\text{CN}}\text{CT}/2)^2 F_{(\text{C,N})\text{amide}}$ are solved for ${}^2J_{\text{CN}}$ and $F_{(\text{C,N})\text{amide}}$, we obtain ${}^2J_{\text{CN}} = 9$ Hz and $F_{(\text{C,N})\text{amide}} = 0.09$. 9 Hz is not too far from the value of ${}^2J_{\text{CN}} = 7.5$ Hz that is typical for coupling of random coil protein C_α's to the amide ^{15}N of the preceding amino acid via the intervening peptide bond (*16*), as in the current case. Neither value of J_{CN} is very precise as the values of CT used were chosen to optimize the experiment's sensitivity to $F_{(\text{C,N})}$ instead. Since the lack of precision in J_{CN} derives from the insensitivity of the sine to variations in its argument near $\pi/2$ but $F_{(\text{C,N})}$ is determined in conjunction with the sine itself, not the argument, the accuracy of $F_{(\text{C,N})}$ is relatively insensitive to the value of J_{CN} with the CT values used.

^{13}C Coupled to ^{15}N in a Minor Product of Acidification

Another ^{13}C^{1}H resonance, C6′ in a minor product of valclavam acidification, was also found to be coupled to ^{15}N (Fig. 5b). For this resonance, the values of $\Delta(\text{control} - J\ \text{coupled})/\text{control}$ obtained with ^{15}N pulses applied at 40 ppm were only 25% of those obtained with ^{15}N pulses at 120 ppm. Thus, the attached ^{15}N appears to resonate at a significantly higher chemical shift than 120 ppm and most likely corresponds to the ^{15}N resonance at 139 ppm in the ^{15}N spectrum (not shown), possibly due to a secondary amide, which would be expected to resonate between 135 and 145 ppm (*36*). Based on frequency profiles of χ, the data acquired with ^{15}N pulses at 120 ppm incorporate only minor off-resonance effects and can be used to estimate that $F_{(\text{C,N})}$ is 0.15, with a coupling constant of ≈9.5 Hz.

CONCLUDING REMARKS

In summary, we have obtained estimates of the fraction of ^{13}C bound to ^{15}N in each of four different $(^1\text{H})^{13}\text{C}-{}^{15}\text{N}$ pairs representing all three N positions in the large fragment of acidified valclavam. Substantial levels of ^{15}N are found in all three N positions, indicating that glycine was extensively metabolized under the fermentation conditions used and its ^{15}N was incorporated into the valine (*3*) and arginine-derived (*1, 2*) portions of valclavam as well as the glycine-like portion. However, ^{13}C labeling is most highly correlated with ^{15}N labeling for positions C10 and N11, with 17% of all ^{13}C-labeled sites being coupled to ^{15}N. Only 12% of labeled C3 is coupled to ^{15}N and similarly for C14 and its attached amine. ^{13}C labeling at C14 is significantly less frequently accompanied by ^{15}N labeling at position N11 than is ^{13}C labeling at position C10, consistent with the fact that C14 is separated by two bonds from N11, so that the two cannot have been labeled by a single intact [2-^{13}C, ^{15}N] fragment derived from glycine. Taking $F_{(\text{C,N})} = 0.09$ for this latter pair as the level of independent co-incorporation of ^{13}C and ^{15}N, approximately 17% − 9% = 8% of the C10–N11 units in valclavam appear to have been derived intact from glycine. The estimate of 9% independent co-incorporation could be further refined by determining the overall percentage of isotope incorporation at each of the N and C positions by quantitative ^{15}N and ^{13}C NMR.

ACKNOWLEDGMENTS

We thank Professor Lewis Kay for generously providing a pulse sequence for CT-HSQC and Cambridge Isotope Labs for the gift of some ^{15}N threonine. A.-F.M. gratefully acknowledges financial support from the N.S.F. MCB-9418181. Thanks are given to the donors of the Petroleum Research Fund, administered by the ACS, for partial support of this research under ACS-PRF 28379-G4. C.A.T. is pleased to thank the N.I.H. for financial support (AI14937). We thank the N.I.H. (RR 06468) for generous financial aid in acquiring the NMR spectrometer used.

REFERENCES

1. J. E. Baldwin, K.-C. Goh, and C. J. Schofield, *Tetrahedron Lett.* **35,** 2779 (1994).
2. D. Iwata-Reuyl and C. A. Townsend, *J. Am. Chem. Soc.* **114,** 2762 (1992).
3. J. W. Janc, L. A. Egan, and C. A. Townsend, *Bioorg. Med. Chem. Lett.* **3,** 2213 (1993).
4. R. A. Brown, R. A. Venters, P.-P. P. Z. Tang, and L. D. Spicer, *J. Magn. Reson. A* **113,** 117 (1995).

5. J. Santoro and G. C. King, *J. Magn. Reson.* **97,** 202 (1992).
6. G. W. Vuister and A. Bax, *J. Magn. Reson.* **98,** 428 (1992).
7. C. Griesinger, O. W. Sørensen, and R. R. Ernst, *J. Chem. Phys.* **85,** 6837 (1986).
8. C. Griesinger, O. W. Sørensen, and R. R. Ernst, *J. Am. Chem. Soc.* **107,** 6394 (1985).
9. V. V. Krishnamurthy, *J. Magn. Reson. A* **114,** 88 (1995).
10. G. Otting, B. A. Messerle, and L. P. Soler, *J. Am. Chem. Soc.* **118,** 5096 (1996).
11. A. Rexroth, P. Schmidt, S. Szalma, O. W. Sørensen, H. Schwalbe, and C. Griesinger, 36th Experimental Nuclear Magnetic Resonance Conference, Abstract P7, Boston, p. 102, March 26–30, 1995.
12. G. W. Vuister, A. C. Wang, and A. Bax, *J. Am. Chem. Soc.* **115,** 5334 (1993).
13. P. R. Blake, B. Lee, M. F. Summers, M. W. W. Adams, J.-B. Park, Z. H. Zhou, and A. Bax, *J. Biomol. NMR* **2,** 527 (1992).
14. S. Grzesiek, G. W. Vuister, and A. Bax, *J. Biomol. NMR* **3,** 487 (1993).
15. A. Rexroth, S. Szalma, R. Weisemann, W. Bermel, H. Schwalbe, and C. Griesinger, *J. Biomol. NMR* **6,** 237 (1995).
16. F. Delaglio, D. A. Torchia, and A. Bax, *J. Biomol. NMR* **1,** 439 (1991).
17. J. R. Tolman and J. H. Prestegard, *J. Magn. Reson. B* **112,** 245 (1996).
18. F. Röhl, J. Rabenhorst, and H. Zähner, *Arch. Microbiol.* **147,** 315 (1987).
19. L. A. Egan, Ph.D. thesis, Johns Hopkins University, Baltimore, 1996.
20. S. P. Salowe, E. N. Marsh, and C. A. Townsend, *Biochemistry* **29,** 6499 (1990).
21. A. E. Bird, J. M. Bellis, and B. C. Gasson, *Analyst* **107,** 1241 (1982).
22. P. K. Glasoe and F. A. Long, *J. Phys. Chem.* **64,** 188 (1960).
23. J. E. Baldwin, T. D. W. Claridge, K.-C. Goh, J. W. Keeping, and C. J. Schofield, *Tetrahedron Lett.* **34,** 5645 (1993).
24. A. Wokaun and R. R. Ernst, *Chem. Phys. Lett.* **52,** 407 (1977).
25. M. Rance, O. W. Sørensen, B. G., G. Wagner, R. R. Ernst, and K. Wuthrich, *Biochem. Biophys. Res. Commun.* **117,** 479 (1983).
26. M. Rance, G. Wagner, O. W. Sørensen, K. Wuthrich, and R. R. Ernst, *J. Magn. Reson.* **59,** 250 (1984).
27. F. J. M. Van de Ven and M. E. P. Philippens, *J. Magn. Reson.* **97,** 637 (1992).
28. D. Marion, M. Ikura, R. Tschudin, and A. Bax, *J. Magn. Reson.* **85,** 393 (1989).
29. L. E. Kay, *Curr. Opin. Struct. Biol.* **5,** 674 (1995).
30. A. Bax and S. Pochapsky, *J. Magn. Reson.* **99,** 638 (1992).
31. A. De Marco, *J. Magn. Reson.* **26,** 527 (1977).
32. G. A. Morris and R. Freeman, *J. Am. Chem. Soc.* **101,** 760 (1979).
33. L. E. Kay, G.-Y. Xu, A. U. Singer, D. R. Muhandiram, and J. D. Forman-Kay, *J. Magn. Reson. B* **101,** 333 (1993).
34. A. Bax, G. M. Clore, P. C. Driscoll, A. M. Gronenborn, M. Ikura, and L. E. Kay, *J. Magn. Reson.* **87,** 620 (1990).
35. A. Bax, M. Ikura, L. E. Kay, G. Barbato, and S. Spera, *in* ''Protein Conformation,'' p. 108, Wiley, Chichester, 1991.
36. G. C. Levy and R. L. Lichter, ''Nitrogen-15 Nuclear Magnetic Resonance Spectroscopy,'' Wiley, New York, 1979.